

Computational Study of 1,3-Dithiane 1,1-Dioxide (1,3-Dithiane Sulfone). Description of the Inversion Process and Manifestation of Stereoelectronic Effects on $^1J_{C-H}$ Coupling Constants

Rafael Notario,^{*,†} María Victoria Roux,[†] Gabriel Cuevas,^{*,‡} Julio Cárdenas,[‡] Verónica Leyva,[‡] and Eusebio Juaristi^{*,§}

Instituto de Química Física Rocasolano, CSIC, Serrano 119, 28006 Madrid, Spain, Instituto de Química, Universidad Nacional Autónoma de México, Cd. Universitaria, Apdo. Postal 70213, 04510 Coyoacán México, D.F., México, and Departamento de Química, Centro de Investigación y de Estudios Avanzados del IPN, Apartado Postal 14-740, 07000 México, D.F., México

Received: January 23, 2006; In Final Form: April 19, 2006

A theoretical study on the conformational interconversions in 1,3-dithiane 1,1-dioxide (1,3-dithiane sulfone) has been carried out. Nineteen conformations have been considered. Four minima and five transition states have been identified. A description of the inversion-topomerization process of 1,3-dithiane sulfone is presented. Calculations show that two transition states are associated with inversion and three more with topomerization. IGLO calculations of the $^1J_{C-H}$ one-bond coupling constants in 1,3-dithiane sulfone have also been carried out. These constants are compared with those obtained for 1,3-dithiane, thiane, and thiane sulfone and their magnitude is explained in terms of stereoelectronic interactions.

Introduction

The conformational properties, geometric parameters and stereoelectronic hyperconjugative interactions of carbocycles and heterocycles are of considerable interest to a wide range of scientists because of the important roles that they play in many areas of science.¹ More than fifty years ago, Barton² published a paper relating cyclohexane conformation to the physical and chemical properties of cyclohexanoid systems. Since then, the conformational analysis of cyclohexane and substituted cyclohexanes, as well as substituted and unsubstituted heterocyclohexanes, has been extensively studied experimentally and computationally.^{1,3–6} There is a large body of information on the chair conformers of substituted saturated six-membered heterocycles but only a few ab initio or density functional theory studies on the mechanisms of conformational interconversions in unsubstituted heterocyclohexanes.⁷ The investigations on substituted saturated six-membered heterocyclohexanes have almost exclusively dealt with possible chair conformers to obtain their geometries, degree of puckering and, in particular, energy differences between axially and equatorially substituted structures.⁴

It is generally accepted that the path for the conformational interconversion of cyclohexane is chair \rightarrow [half-chair/sofa] ‡ \rightarrow twist \rightarrow [boat] ‡ \rightarrow twist \rightarrow [half-chair/sofa] ‡ \rightarrow chair, with the free energy of activation of inversion being associated with the step chair \rightarrow [half-chair/sofa] ‡ . This barrier is in the range 40–45 kJ mol⁻¹.^{7a}

Over the past few years, we have been involved⁸ in the systematic experimental and theoretical thermochemical study of selected sulfur six-membered heterocycles: 1,3-dithiane,^{8a,b} 1,4-dithiane,^{8b} 1,3,5-trithiane,^{8c} thiane sulfone,^{8d} thiane sulfoxide,^{8d}

TABLE 1: B3LYP/6-311+G(d,p) Thermochemical Data for Conformers and Transition States of 1,3-Dithiane Sulfone

species	B3LYP/6-311+G(d,p)			
	E_{el}^a	ZPE ^b	TCH ^c	S^d
chair, 1	-1104.151203	0.123624	0.132623	367.81
1,4-twist, 2	-1104.146903	0.123609	0.132736	372.50
2,5-twist, 3	-1104.145538	0.123656	0.132828	374.47
3,6-twist, 4	-1104.143321	0.123717	0.132870	375.69
1,4-boat, [5] ‡	-1104.141363	0.123631	0.132065	358.36
2,5-boat, [6] ‡	-1104.143277	0.123562	0.131876	355.39
3,6-boat, [7] ‡	-1104.145119	0.123448	0.131847	357.71
[TS-1] ‡	-1104.137556	0.123522	0.132016	363.29
[TS-2] ‡	-1104.138063	0.123457	0.131933	361.04

^a Electronic energies, in Hartrees. ^b Zero-point vibrational energies, in Hartrees. ^c Thermal correction to enthalpies, in Hartrees. ^d Entropies in J mol⁻¹ K⁻¹.

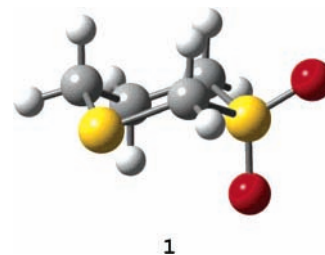


Figure 1. Chair conformation of 1,3-dithiane sulfone.

1,3-dithiane sulfone,^{8c} and 1,3-dithiane sulfoxide.^{8f} In this work, we have carried out a theoretical study on the conformational interconversions in 1,3-dithiane 1,1-dioxide (1,3-dithiane sulfone), investigating the possible stereoelectronic hyperconjugative interactions in various conformers and transition states.

Computational Methods

All calculations were carried out with Spartan'04⁹ and Gaussian03¹⁰ programs. All the minima and transition states

* Corresponding author. Tel: 34 91 561 94 00. Fax: 34 91 564 24 31. E-mail: rnotario@iqfr.csic.es.

[†] CSIC.

[‡] Universidad Nacional Autónoma de México.

[§] Centro de Investigación y de Estudios Avanzados del IPN.

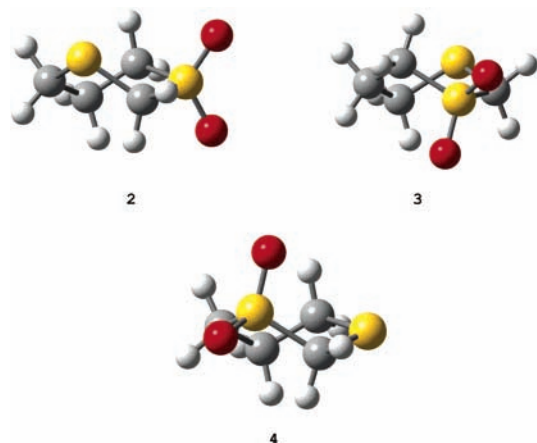


Figure 2. 1,4-Twist (**2**), 2,5-twist (**3**), and 3,6-twist (**4**) conformations of 1,3-dithiane sulfone.

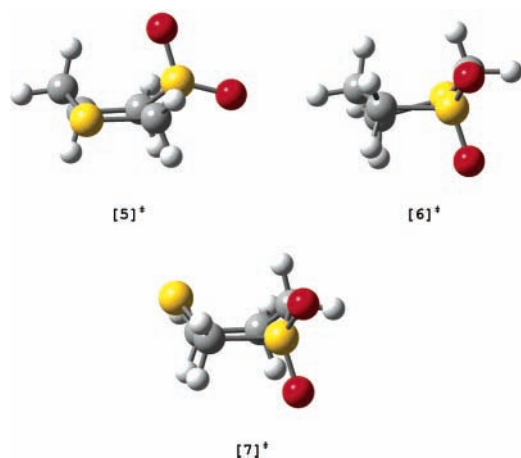


Figure 3. 1,4-Boat (**[5][‡]**), 2,5-boat (**[6][‡]**), and 3,6-boat (**[7][‡]**) conformations of 1,3-dithiane sulfone.

were fully optimized at the B3LYP/6-311+G(d,p) level of theory. The B3LYP model¹¹ is the combination of Becke's three-parameter hybrid exchange functional¹² with the Lee, Yang and Parr (LYP) correlation functional.¹³ The basis used was 6-311G,^{14,15} including polarization and diffuse functions.¹⁶ We have used density functional theory (DFT) because it provides electron correlation, which is often important in conformational studies.¹⁷ Diffuse functions are important for molecules with a lone pair of electrons, and polarization functions have been useful in computational studies involving hyperconjugative stereoelectronic interactions and involving structures containing third row elements.^{7g}

Frequency calculations were carried out at the same level of theory. The zero-point vibrational energies were scaled by the factor 0.9806.¹⁸

Intrinsic reaction coordinate, IRC, calculations¹⁹ at the B3LYP/6-311+G(d,p) level of theory were carried out on the optimized transition states to obtain the two minima on the potential energy surface, PES, connected by each transition state.

The B3LYP/6-311+G(d,p)-calculated electronic energies, zero-point vibrational energies, thermal correction to enthalpies, and entropies for all the minima and transition states involved in the conformational interconversion of 1,3-dithiane sulfone are given in Table 1.

BP/IGLO-III/B3LYP/6-311++G(2d,2p) calculations of the $^1J_{C-H}$ one-bond coupling constants of 1,3-dithiane sulfone have also been carried out.

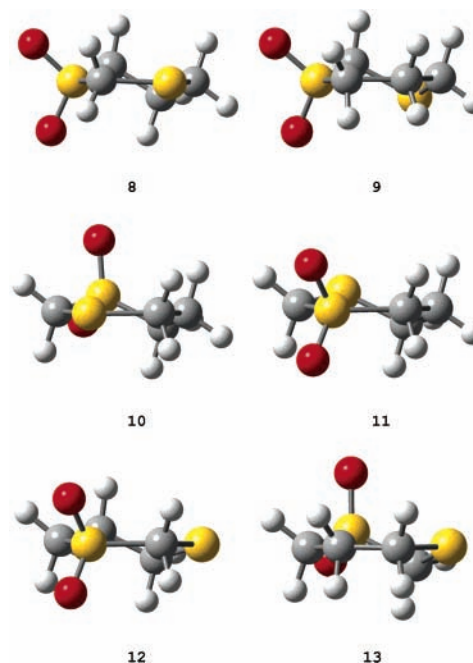


Figure 4. 1,4-Half-chair (**8** and **9**), 2,5-half-chair (**10** and **11**), and 3,6-half-chair (**12** and **13**) conformations of 1,3-dithiane sulfone.

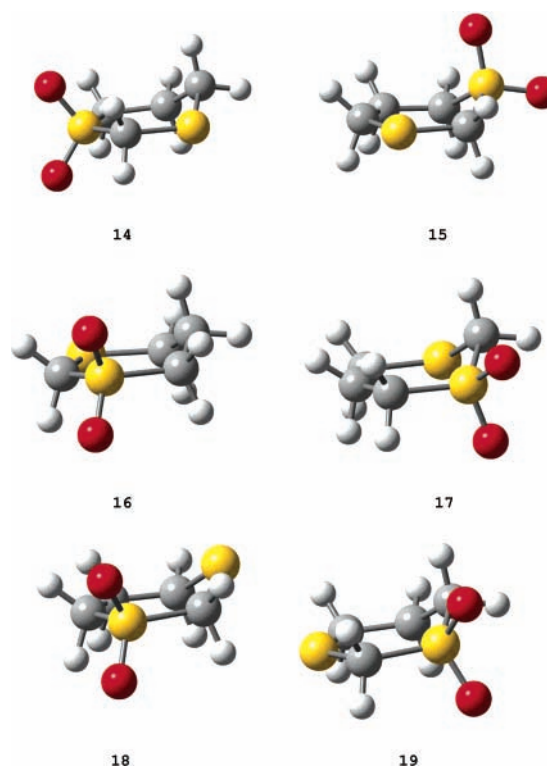


Figure 5. 1,4-Sofa (**14** and **15**), 2,5-sofa (**16** and **17**), and 3,6-sofa (**18** and **19**) conformations of 1,3-dithiane sulfone.

Results and Discussion

A. Conformational Interconversion. By analogy with cyclohexane and the six-membered heterocyclic rings,⁷ there are 19 conformations to be considered for the conformational interconversion of 1,3-dithiane sulfone. All of them are shown in Figures 1–5.

Vibrational frequency calculations identified four stationary states of minimum energy: chair, **1** (see Figure 1), and the three twist conformers 1,4-twist, **2**, 2,5-twist, **3**, and 3,6-twist, **4** (see Figure 2); and three transition states, the three boat conformers

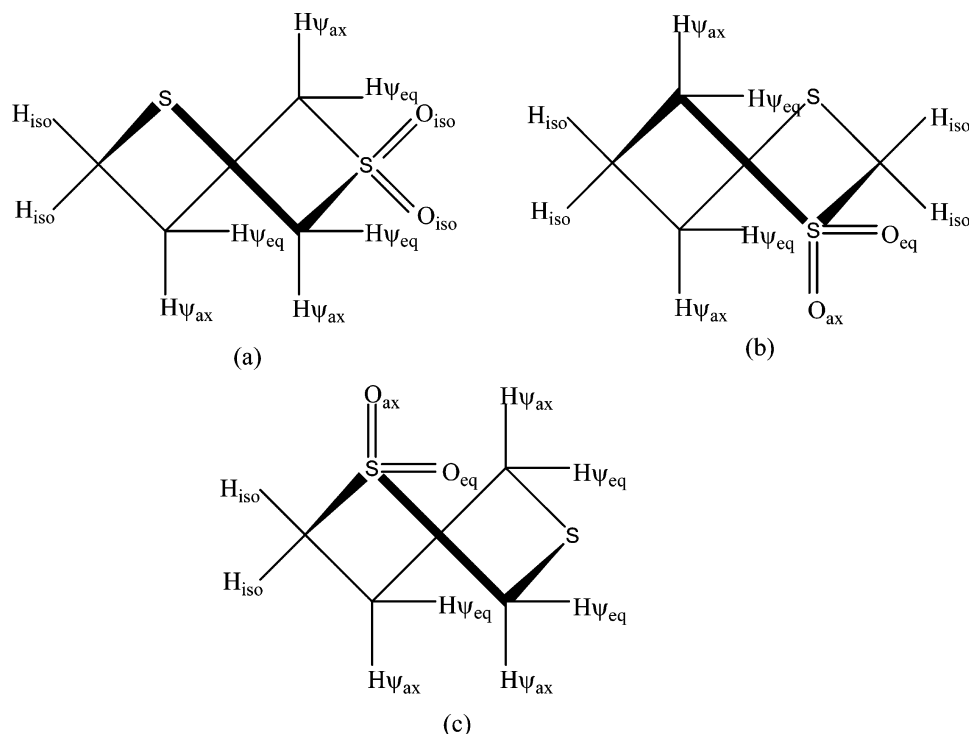


Figure 6. Positions of the substituents in 1,4-twist (a), 2,5-twist (b) and 3,6-twist (c) conformers of 1,3-dithiane sulfone.

TABLE 2: Bond Lengths, in Ångstroms, for the Chair Conformer, **1**, of 1,3-Dithiane Sulfone, Calculated at the B3LYP/6-311+G(d,p) Level

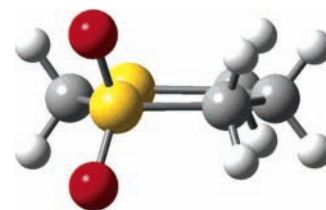
S ₁ –C ₂	1.833
C ₂ –S ₃	1.814
S ₃ –C ₄	1.837
C ₄ –C ₅	1.531
C ₅ –C ₆	1.532
C ₆ –S ₁	1.820
S ₁ –O _{ax}	1.466
S ₁ –O _{eq}	1.469
C ₂ –H _{ax}	1.092
C ₂ –H _{eq}	1.090
C ₄ –H _{ax}	1.094
C ₄ –H _{eq}	1.091
C ₅ –H _{ax}	1.093
C ₅ –H _{eq}	1.096
C ₆ –H _{ax}	1.093
C ₆ –H _{eq}	1.092

1,4-boat, **[5]**[‡], 2,5-boat, **[6]**[‡], and 3,6-boat, **[7]**[‡] (see Figure 3). The calculated bond lengths for the chair and the three twist conformers are given in Tables 2 and 3. It has to be noted that in the case of twist conformations there are three possible positions for the substituents: pseudoaxial (ψ_{ax}), pseudoequatorial (ψ_{eq}), and isoclinal (iso) (see Figure 6).

The chair conformer is 11.3, 14.9 and 20.7 kJ mol⁻¹, respectively, more stable than the 1,4-twist, 2,5-twist and 3,6-twist conformers. The thermodynamic parameters for conformers and transition states of 1,3-dithiane sulfone relative to the most stable chair conformer are given in Table 4.

There are also six possible half-chair structures (see Figure 4): the 1,4-half-chairs, **8** and **9**, the 2,5-half-chairs, **10** and **11**, and the 3,6-half-chairs, **12** and **13**; and six sofa structures (see Figure 5): the 1,4-sofas, **14** and **15**, the 2,5-sofas, **16** and **17**, and the 3,6-sofas, **18** and **19**. The hypothetical high energy planar form (see Figure 7), **20**, is not expected to be involved in the conformational interconversion mechanisms.

All the half-chair and sofa structures are not minima on the potential energy surface. Two transition structures, **[TS-1]**[‡] and



20

Figure 7. Hypothetical planar conformation of 1,3-dithiane sulfone.

TABLE 3: Bond Lengths, in Ångstroms, for the Three Twist Conformers of 1,3-Dithiane Sulfone, Calculated at the B3LYP/6-311+G(d,p) Level

	1,4-twist, 2	2,5-twist, 3	3,6-twist, 4
S ₁ –C ₂	1.846	1.853	1.829
C ₂ –S ₃	1.809	1.824	1.820
S ₃ –C ₄	1.849	1.839	1.850
C ₄ –C ₅	1.539	1.541	1.530
C ₅ –C ₆	1.530	1.535	1.536
C ₆ –S ₁	1.830	1.816	1.837
S ₁ –O ψ_{ax}		1.471	1.466
S ₁ –O ψ_{eq}		1.467	1.468
S ₁ –O _{iso}	1.465/1.470		
C ₂ –H ψ_{ax}	1.090		1.091
C ₂ –H ψ_{eq}	1.090		1.090
C ₂ –H _{iso}		1.089/1.091	
C ₄ –H ψ_{ax}		1.091	1.092
C ₄ –H ψ_{eq}		1.090	1.090
C ₄ –H _{iso}	1.091/1.092		
C ₅ –H ψ_{ax}	1.094		1.094
C ₅ –H ψ_{eq}	1.094		1.095
C ₅ –H _{iso}		1.092/1.094	
C ₆ –H ψ_{ax}	1.090	1.090	
C ₆ –H ψ_{eq}	1.091	1.092	
C ₆ –H _{iso}			1.090/1.092

[TS-2][‡], were obtained from the half-chair and sofa structures (see Figure 8). **[TS-1]**[‡] was obtained from structures **8**, **10**, **12**, **13**, **16** and **19**, and **[TS-2]**[‡] was obtained from structures **9**, **11**, **15**, **17** and **18**.

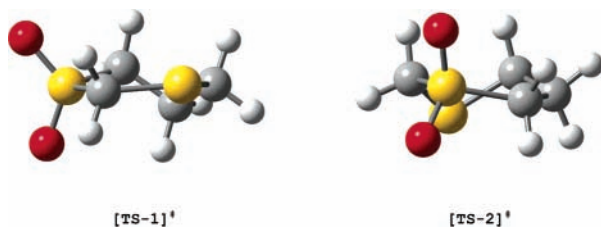


Figure 8. Transition structures obtained from the half-chair and sofa conformations of 1,3-dithiane sulfone.

TABLE 4: Thermodynamic Parameters (kJ/mol; Relative to the Chair Conformer) for Conformers and Transition States of 1,3-Dithiane Sulfone

	B3LYP/6-311+G(d,p)			
	ΔE_{el}	ΔE_0	ΔH_{298}	ΔG_{298}
1,4-twist, 2	11.3	11.3	11.6	10.2
2,5-twist, 3	14.9	15.0	15.4	13.4
3,6-twist, 4	20.7	20.9	21.3	19.0
1,4-boat, [5] [‡]	25.8	25.9	24.4	27.2
2,5-boat, [6] [‡]	20.8	20.6	18.9	22.6
3,6-boat, [7] [‡]	16.0	15.5	13.9	17.0
[TS-1] [‡]	35.8	35.6	34.2	35.6
[TS-2] [‡]	34.5	34.1	32.7	34.7

IRC calculations at the B3LYP/6-311+G(d,p) level were carried out to determine the two minima connected by the corresponding transition structure. The respective geometries of the 1,4-boat, [**5**][‡], 2,5-boat, [**6**][‡], and 3,6-boat, [**7**][‡], transition states were essentially unchanged after attempted IRC calculations. A similar behavior in the case of transition states derived from boat structures has been observed in the study of thiane,^{7e} 1,3-dithiane,^{7g} 1,2,3-trithiane,^{7h} or 3-silathiacyclohexane.⁷ⁱ Although it is qualitative, the animated displacements at the imaginary frequencies permit us to establish what conformers are connected by the TS. So, the animated displacements at 95.11 cm⁻¹ for 1,4-boat, [**5**][‡], suggest that it is the barrier to the interconversion of the conformers 2,5-twist, **3**, and 3,6-twist, **4**. Similarly, the animated displacements at 43.81 cm⁻¹ for 2,5-

boat, [**6**][‡], suggest that it is the barrier to the interconversion of the conformers 1,4-twist, **2**, and 3,6-twist, **4**, and those at 60.71 cm⁻¹ for 3,6-boat, [**7**][‡], suggest that it is the barrier to the interconversion of the conformers 1,4-twist, **2**, and 2,5-twist, **3**.

IRC calculations on transition state [**TS-1**][‡] at the B3LYP/6-311+G(d,p) level of theory connected the chair, **1**, and 1,4-twist, **2**, conformers (see Figure 9); and IRC calculations on transition state [**TS-2**][‡] at the same level of theory connected the chair, **1**, and 2,5-twist, **3**, conformers (see Figure 10). The free energy diagram for the chair-chair interconversion of 1,3-dithiane sulfone is shown in Figure 11.

We have recently stated²⁰ that the conformational process, being a dynamic phenomenon, cannot be satisfactorily described in terms of isolated stationary states. Therefore, it is necessary to describe it in terms of a group of elementary conformational stages constituted by a transition state and the two minima it connects,²¹ similar to the elementary stages used to describe reaction mechanisms.²² Figure 12 shows the inversion process of chair **1**.

Similar to what has been observed in the case of oxane and thiane,²¹ there are two independent processes that share two common intermediaries. The annular inversion process is controlled by two transition states ([**TS-1**][‡] and [**TS-2**][‡], Figure 12) that are found at 35.8 and 34.5 kJ mol⁻¹ of the chair. It is interesting to point out that this value is smaller than that required for annular inversion of cyclohexane (42.9 kJ mol⁻¹ at 213 to 223 K),¹ or oxane (43.1 kJ mol⁻¹ at 212 K),²³ but is closer to the inversion energy in thiane (39.3 kJ mol⁻¹ at 192 K),²³ or 1,3-dithiane (39.3 kJ mol⁻¹ at 193 K).²⁴ In comparison to the other systems described where the heteroatom and methylene at position 4 control the inversion process, the sulfone of 1,3 dithiane, the methylenes at position 2 and position 5 control annular inversion as shown on transition states [**TS-1**][‡] and [**TS-2**][‡], respectively.

The barriers required by skewed boats **3** and **4** to reach transition states **7** and **6** respectively are very small (1.1 y 0.1

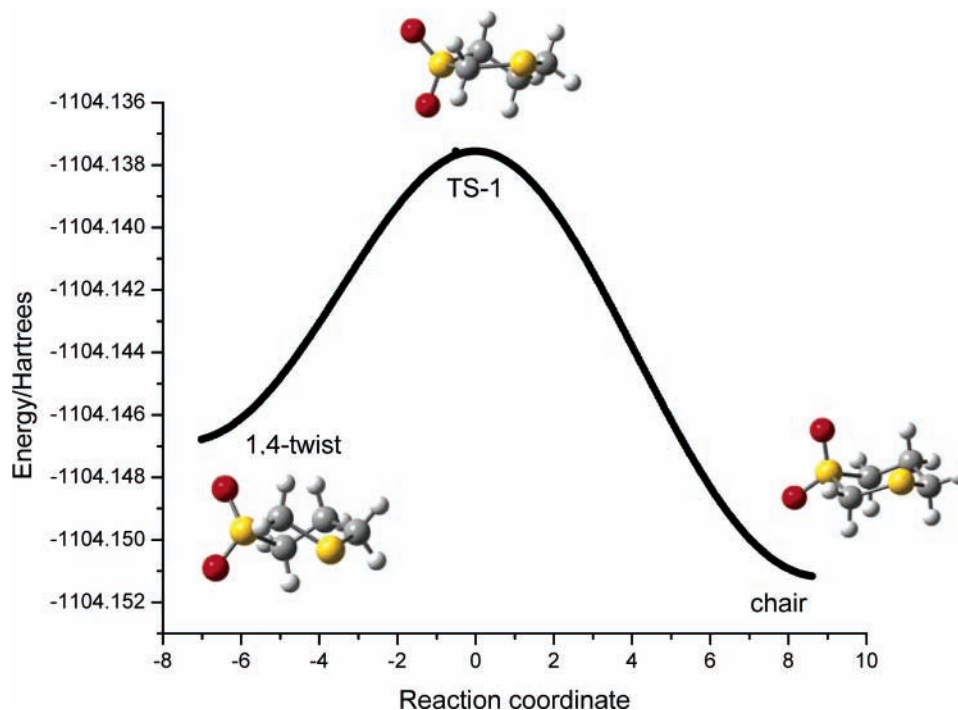


Figure 9. IRC calculations at the B3LYP/6-311+G(d,p) level connecting chair and 1,4-twist conformers of 1,3-dithiane sulfone through the TS-1 transition state.

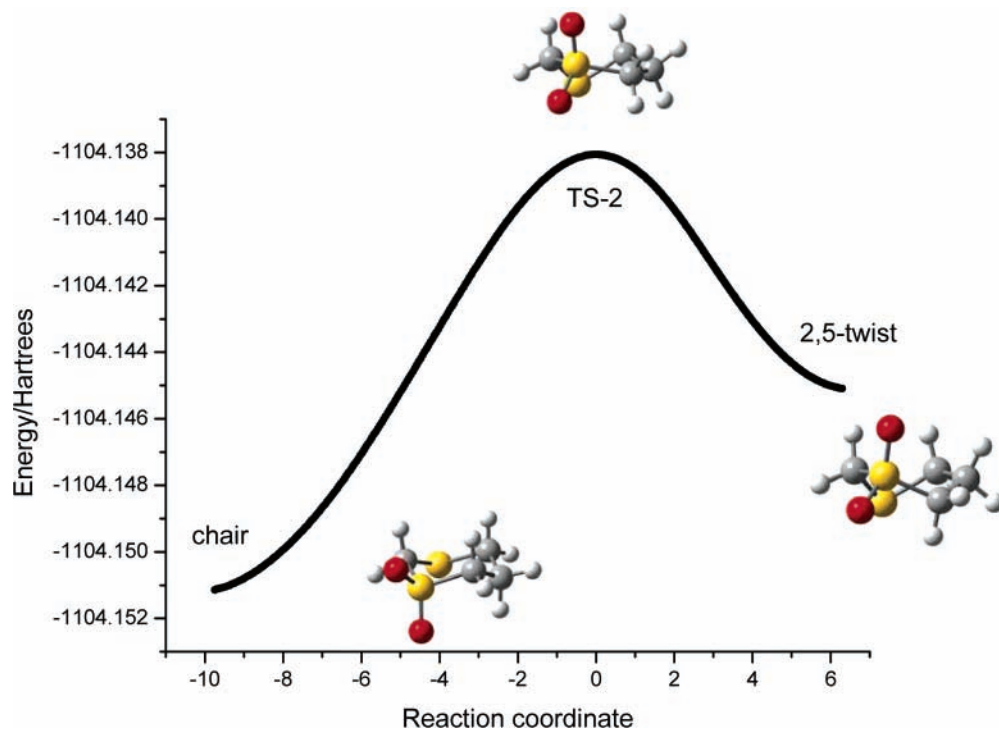


Figure 10. IRC calculations at the B3LYP/6-311+G(d,p) level connecting chair and 2,5-twist conformers of 1,3-dithiane sulfone through the TS-2 transition state.

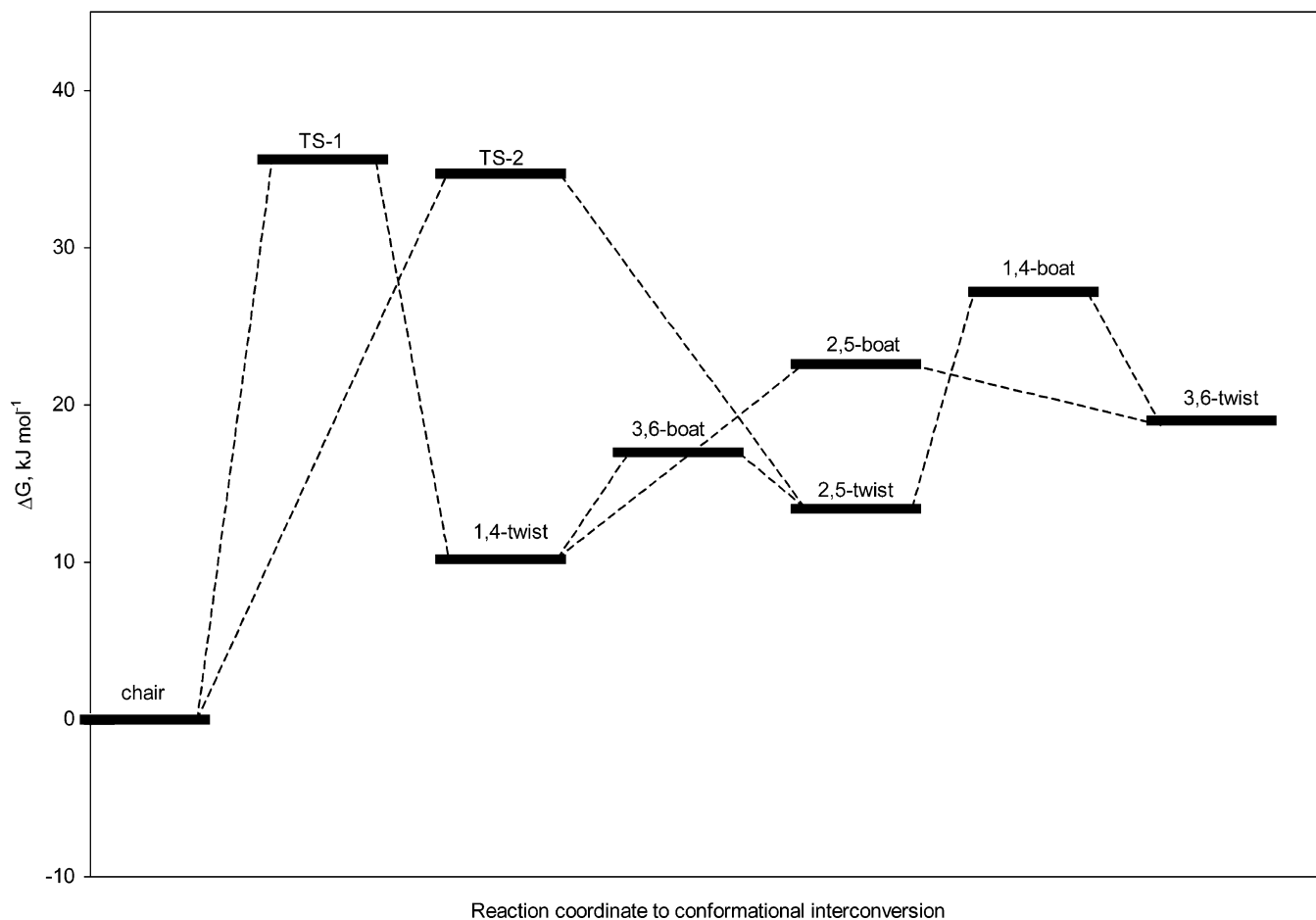


Figure 11. Free energy diagram for the chair-chair interconversion of 1,3-dithiane sulfone.

kJ mol^{-1}). The barriers associated with skewed boats **2** and **4** when transition states **7** and **5** are reached can also be considered low (4.7 and 5.1 kJ mol^{-1} , respectively). However, for boats **3**

and **2** to reach transition states **5** and **6**, 10.9 and 9.5 kJ mol^{-1} are needed. These barriers are unusually high for a topomerization process and will certainly have an impact on the entropy

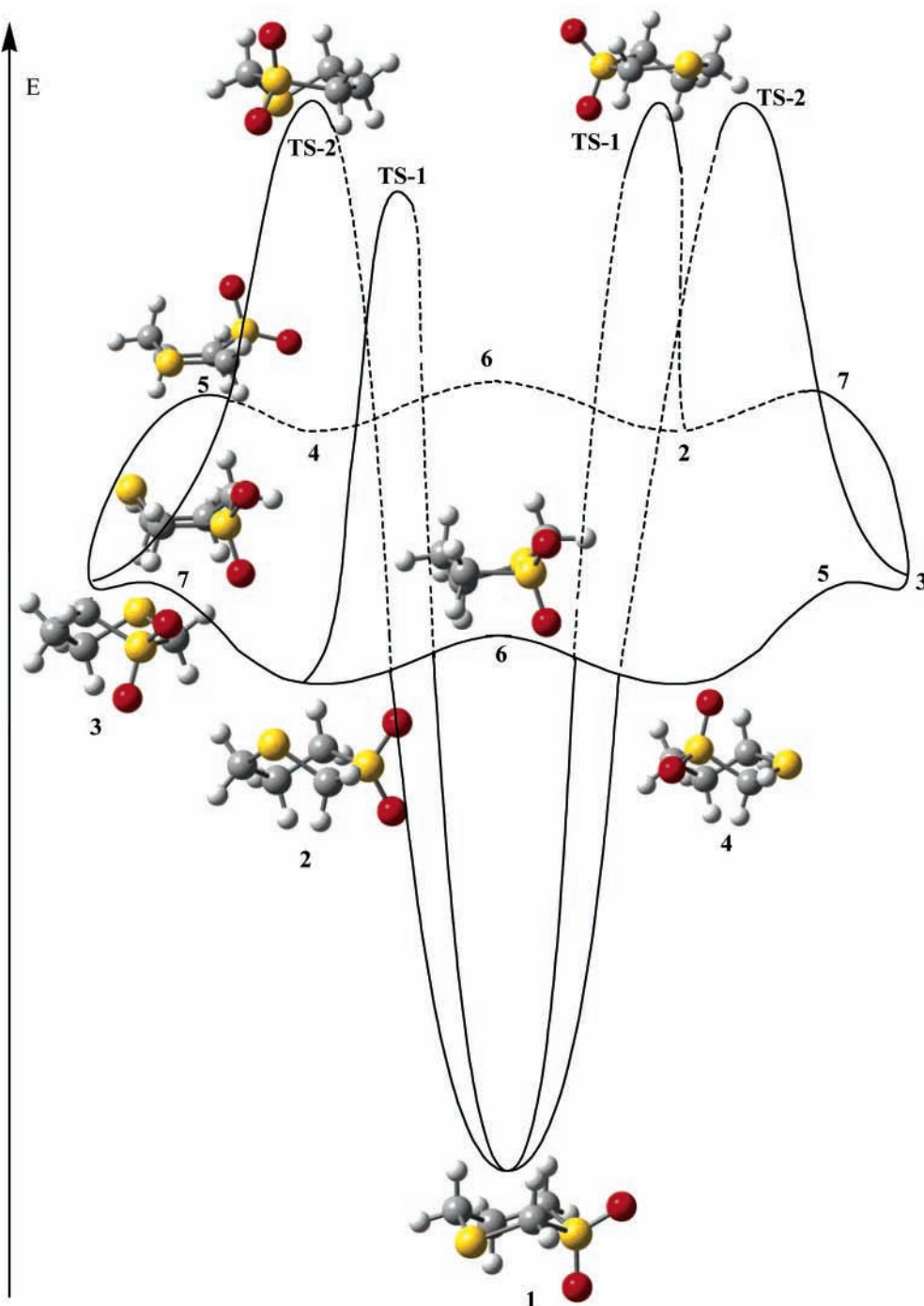


Figure 12. Topomerization and inversion processes in 1,3-dithiane sulfone.

of the system. The rest of the stationary states that can be optimized lack physical sense.

B. Manifestation of Stereoelectronic Interactions on the Magnitude of $^1J_{C-H}$ One-Bond Coupling Constants. The seminal contributions for the development of the useful correlation between C–H bond orientation and the magnitude of the corresponding $^1J_{C-H}$ one bond coupling constant are due to Perlin and Casu.²⁵ Most appropriately, Wolfe et al. proposed²⁶ some years ago that stereoelectronic effects upon one-bond C–H coupling constants be termed “Perlin effects”.

In particular, the magnitude of the one-bond C–H coupling constant for an axial C–H bond adjacent to oxygen or nitrogen in a six-membered ring is smaller by 8–18 Hz relative to $^1J_{C-H}$ in the corresponding equatorial bond, i.e., $^1J_{C-Heq} > ^1J_{C-Hax}$ (see Figure 13a). This situation represents a “normal” Perlin effect

(NPE in this paper, $\Delta^1J_{C-H} = ^1J_{C-Heq} - ^1J_{C-Hax} > 0$) and is usually interpreted in terms of an $n_X \rightarrow \sigma^*_{C-Hax}$ ($X = O, N$) interaction between a pair of nonbonded electrons on oxygen or nitrogen and the axial (antiperiplanar) adjacent C–H_{ax} bond,²⁷ that weakens such bond and results in smaller coupling constants (see Figure 13b).

In contrast, sulfur-containing 1,3-dithiane analogues have been shown²⁸ to exhibit an opposite behavior: $^1J_{Ceq} < ^1J_{Cax}$, which now represents a “reverse” Perlin effect (RPE in this paper, $\Delta^1J_{C-H} = ^1J_{C-Heq} - ^1J_{C-Hax} < 0$, Figure 13c). This reversal of the relative magnitude of the coupling constants in 1,3-dithianes was explained by Wolfe et al.^{26,29} as a result of dominant $\sigma_{C-S} \rightarrow \sigma^*_{C-Heq}$ (rather than $n_S \rightarrow \sigma^*_{C-Hax}$) interaction (Figure 13d).

In the present work, theoretical calculation of the optimized structure [B3LYP/6-311++G(2d,2p)] of 1,3-dithiane sulfone,

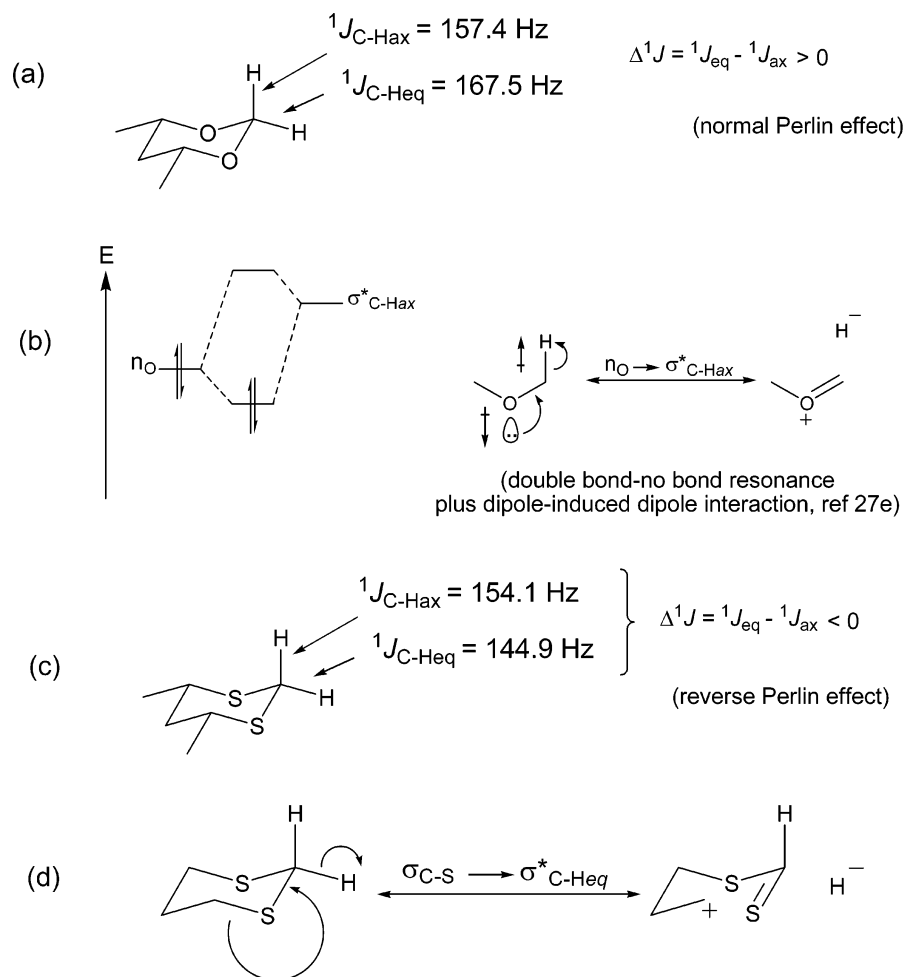


Figure 13. Normal Perlin effect in oxygen-containing six-membered ring heterocycles and reverse Perlin effect in 1,3-dithianes.

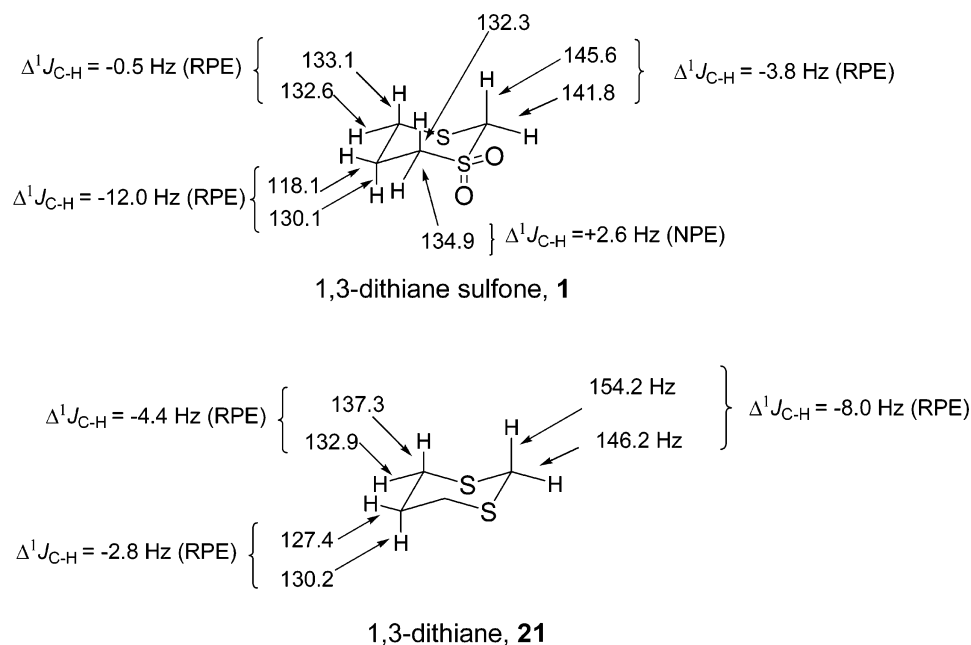


Figure 14. Experimental $^1J_{C-H}$ one-bond coupling constants measured for 1,3-dithiane **21**, and calculated $^1J_{C-H}$ one-bond coupling constants for 1,3-dithiane sulfone **1**.

1, was followed by estimation of the $^1J_{C-H}$ one-bond coupling constants [BP/IGLO-III/B3LYP/6-311++G(2d,2p)].³⁰ Figure 14 collects the calculated data for all C-H one-bond coupling constants in **1**, which includes for comparison purposes the values obtained experimentally for 1,3-dithiane, **21**.^{28b,c}

It is anticipated that the σ_{C-SO_2} orbital in sulfone **1** will not be as effective donor relative to the donor σ_{C-S} orbital in 1,3-dithiane **21**.

To facilitate the comparison of data in **1** and **21**, Figure 15 collects the calculated $^1J_{C-H}$ one-bond coupling constants for

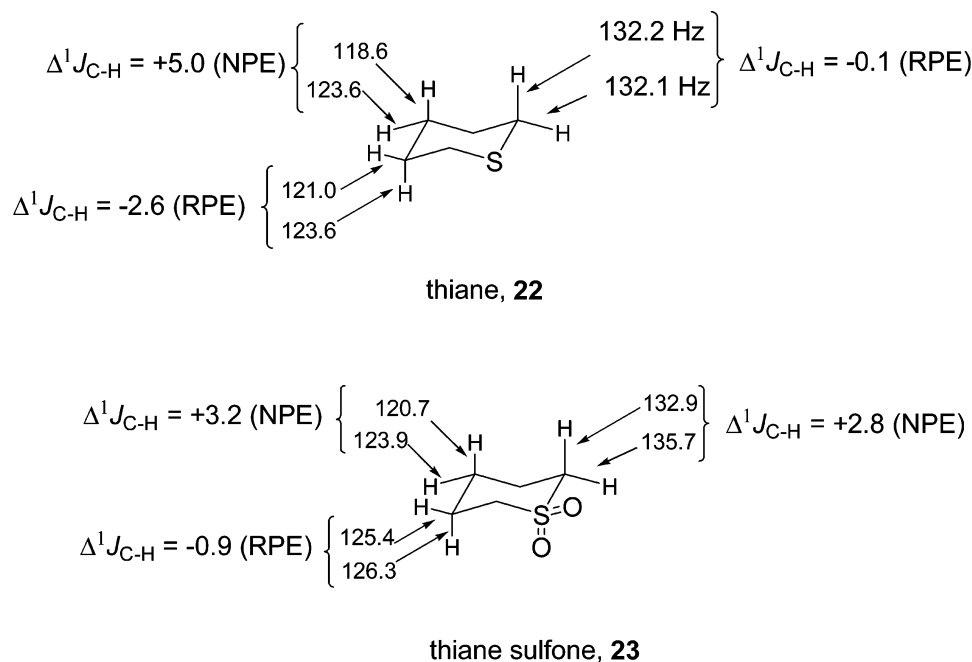


Figure 15. Calculated [BP/IGLO-III/B3LYP/6-311G++(2d,2p)] coupling constants in thiane **22** (ref 31) and thiane sulfone **23** (this work).

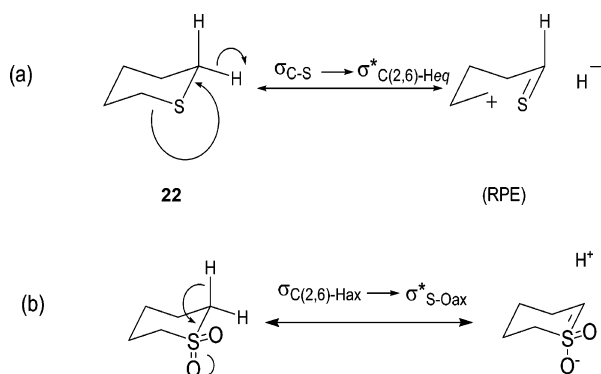


Figure 16. Dominant stereoelectronic interactions operative in thiane **22** (RPE, $\Delta^1J_{C(2,6)-H} = -0.1$ Hz) and thiane sulfone **23** (NPE, $\Delta^1J_{C(2,6)-H} = +2.8$ Hz).

thiane, **22**, in ref 31, as well as the calculated (this work) $^1J_{C-H}$ one-bond coupling constants in thiane sulfone, **23**.

Salient observations from the comparison of the calculated $^1J_{C-H}$ one-bond coupling constants presented in Figure 15 follow:

(1) The reverse Perlin effect (RPE) operative at C(2,6) in thiane **22** ($\Delta^1J_{C-H} = -0.1$ Hz) is in contrast with the normal Perlin effect (NPE) observed for the same methylene C–H bonds α to the sulfonyl group in thiane sulfone **23** ($\Delta^1J_{C-H} = +2.8$ Hz). It is apparent then that the dominant $\sigma_{C-S} \rightarrow \sigma^*_{C(2,6)-Heq}$ stereoelectronic interaction that weakens the equatorial C–H bonds adjacent to sulfur in thiane **22**^{26,28,31} (Figure 16a) is overcome by $\sigma_{C(2,6)-Hax} \rightarrow \sigma^*_{S-Oax}$ delocalization³² in thiane sulfone **23**, weakening the axial C(2,6)–H_{ax} bonds and resulting in the observed NPE (Figure 16b).

(2) The substantial RPE ($\Delta^1J_{C(3,5)-H} = -2.6$ Hz) found at the β methylenes in thiane **22** dwindles significantly in thiane sulfone **23** ($\Delta^1J_{C(3,5)-H} = -0.9$ Hz), owing to the diminished donor ability of the σ_{C-SO_2} orbitals relative to σ_{C-S} donor orbitals. Thus, C(3,5)–H_{eq} presents a larger $^1J_{C-H}$ one-bond coupling constant in the sulfone, from 121.90 Hz in **22** to 125.4 Hz in **23**.

(3) No significant change in the values of the C–H one bond coupling constants is appreciated at the more distant (relative to the sulfur group) gamma methylene.

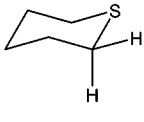
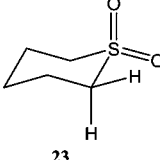
Interpretation of the $^1J_{C-H}$ One-bond Coupling Constants Calculated in 1,3-Dithiane Sulfone, **1.** The information collected in Figures 15 and 16 facilitates the interpretation of the C–H one-bond coupling constants calculated for 1,3-dithiane sulfone **1** (Figure 14).

(1) At C(2), the methylene group adjacent to both the thioether and sulfonyl sulfur atoms, the large RPE ($\Delta^1J_{C(2)-H} = -8.0$ Hz) encountered in 1,3-dithiane **21** diminishes significantly to ($\Delta^1J_{C(2)-H} = -3.8$ Hz). This observation can be explained in terms of the loss in sulfone **1** of one of the two $\sigma_{C(2)-H_{eq}} \rightarrow \sigma^*_{C(2)-Heq}$ interactions that weaken the equatorial C(2)–H bond in 1,3-dithiane,^{26,28,31} and the simultaneous participation of $\sigma_{C(2)-H_{ax}} \rightarrow \sigma^*_{S-O_{ax}}$ delocalization,³² that weakens the axial C–H bond in the sulfone.

As was recently shown by Alabugin,³³ the natural bond orbitals (NBO) method developed by Weinhold and co-workers is a very useful theoretical method for the study of hyperconjugative interactions.³⁴ In particular, NBO analysis gives the energies of the delocalizing interactions that are weakening the C–H bonds of interest. These energies (E_{del}) are obtained by the deletion of the corresponding Fock elements and followed by the recalculation of the wave function.^{33a}

Table 5 summarizes the NBO-estimated energies of deletion (E_{del}) for the main hyperconjugative interactions in thiane **22** and thiane sulfone **23**. Table 5 includes the calculated difference in energy between the donor and acceptor orbitals of interest. As anticipated, the magnitude of the two-electron/two-orbital hyperconjugative interaction depends inversely on the energy gap between the donor and acceptor orbitals. Thus, as evidenced by the analysis of the C–H bond strength presented above in terms of the relative magnitude of one-bond coupling constants, the small energy difference encountered between the donor $\sigma_{C(2,6)-H_{ax}}$ and acceptor $\sigma^*(S-O_{ax})$ orbitals in thiane sulfone **6** ($\Delta E = 0.82$ Hartrees) results in a substantial delocalizing interaction ($E_{del} = 2.27$ kcal mol⁻¹). In contrast, although the calculated energy difference between the potentially donor

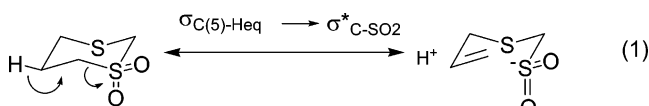
TABLE 5: Selected Hyperconjugative Interactions (E_{del}) for C–H Bonds Adjacent to Sulfur in Thiane **22 and Thiane Sulfone **23****

	donor orbital	acceptor orbital	E_{del} (kcal/mol)	$\Delta E_{\text{donor/acceptor}}$ (Hartrees)
	$\sigma_{\text{C}(2,6)\text{-Hax}}$	$\sigma^*_{\text{C}(3,5)\text{-Hax}}$	2.52	0.97
	$\sigma_{\text{C}(2,6)\text{-Hax}}$	$\sigma^*_{\text{S-Oax}}$	2.27	0.82
	$\sigma_{\text{C}(2,6)\text{-Hax}}$	$\sigma^*_{\text{C}(3,5)\text{-Hax}}$	2.24	0.99
	$\sigma_{\text{C}(2,6)\text{-Hax}}$	$\sigma^*_{\text{S-Oeq}}$	0.39	0.98
	$\sigma_{\text{C}(2,6)\text{-Heq}}$	$\sigma^*_{\text{S-Oax}}$	0.31	0.82

equatorial C–H orbital $\sigma_{\text{C}(2,6)\text{-Heq}}$ and acceptor $\sigma^*(\text{S}=\text{O}_{\text{ax}})$ is equally small ($\Delta E = 0.82$ Hartrees) the delocalization interaction is negligible ($E_{\text{del}} = 0.31$ kcal mol⁻¹), as a consequence of the unfavorable orbital orientation, i.e., gauche rather than antiperiplanar.

(2) At C(4), that is the methylene group adjacent to the thioether sulfur in **1**, the RPE is substantially reduced, from $\Delta^1J_{\text{C}(4)\text{-H}} = -4.4$ Hz in 1,3-dithiane **21** to $\Delta^1J_{\text{C}(4)\text{-H}} = -0.5$ Hz in sulfone **1**. It seems likely that electron density at the donor S(3) sulfide atom is partially depleted as a consequence of $n_{\text{S}} \rightarrow \sigma^*_{\text{C}-\text{SO}_2}$ delocalization,^{8e,35} so that $\sigma_{\text{C}(2)\text{-S}} \rightarrow \sigma^*_{\text{C}(4)\text{-Heq}}$ dwindles and as a result the final RPE is smaller.

(3) At C(5), unexpectedly the magnitude of the one-bond $^1J_{\text{C-Heq}}$ decreases substantially, from 127.4 Hz in 1,3-dithiane **21** to 118.1 Hz in 1,3-dithiane sulfone **1**. This observation is readily understood in terms of $\sigma_{\text{C}(5)\text{-Heq}}$ to $\sigma^*_{\text{C}-\text{SO}_2}$ delocalization (eq 1).



(4) At C(6), that is the methylene group adjacent to the sulfonyl group, the observed NPE = +2.6 Hz contrasts sharply with the RPE = -4.4 Hz reported for 1,3-dithiane **21**. This interesting observation is in line with loss of $\sigma_{\text{C-S}} \rightarrow \sigma^*_{\text{C}(6)\text{-Heq}}$ hyperconjugation and simultaneous $\sigma_{\text{C}(6)\text{-Hax}} \rightarrow \sigma^*_{\text{S-Oax}}$ delocalization in 1,3-dithiane sulfone **1**.

Acknowledgment. The support of the Spanish DGI under Projects QU2003-05827 and FIS2004-02954-C03-01 is gratefully acknowledged. E.J. is indebted to Conacyt (México) for financial support via grant 45157.

References and Notes

- (1) Eliel, E. L.; Wilen, S. H. *Stereochemistry of Organic Compounds*; Wiley: New York, 1994; Chapter 11 and references therein.
- (2) Barton, D. H. R. *Experientia* **1950**, *6*, 316–320.
- (3) *Conformational Behavior of Six-membered Rings*; Juaristi, E., Ed.; VCH Publishers: New York, 1995.
- (4) Bushweller, C. H. In *Conformational Behavior of Six-membered Rings*; Juaristi, E., Ed.; VCH Publishers: New York, 1995; Chapter 2 and references therein.
- (5) Cremer, D.; Szabo, K. J. In *Conformational Behavior of Six-membered Rings*; Juaristi, E., Ed.; VCH Publishers: New York, 1995; Chapter 3 and references therein.
- (6) Kleinpeter, E. In *Conformational Behavior of Six-membered Rings*; Juaristi, E., Ed.; VCH Publishers: New York, 1995; Chapter 6 and references therein.
- (7) (a) Chapman, D. M.; Hester, R. E. *J. Phys. Chem. A* **1997**, *101*, 3382–3387. (b) Freeman, F.; Kasner, M. L.; Hehre, W. J. *J. Phys. Chem. A* **2001**, *105*, 10123–10132. (c) Freeman, F.; Do, K. U. *J. Mol. Struct.*

(*THEOCHEM*) **2002**, *577*, 43–54. (d) Freeman, F.; Lee, K.; Hehre, W. J. *Struct. Chem.* **2002**, *13*, 149–160. (e) Freeman, F.; Derek, E. *Struct. Chem.* **2003**, *14*, 497–510. (f) Freeman, F.; Derek, E. *J. Comput. Chem.* **2003**, *24*, 909–919. (g) Freeman, F.; Le, K. T. *J. Phys. Chem. A* **2003**, *107*, 2908–2918. (h) Freeman, F.; Cha, C. *J. Phys. Org. Chem.* **2004**, *17*, 32–41. (i) Freeman, F.; Cha, C.; Fang, C.; Huang, A. C.; Hwang, J. H.; Shaiyuan, B. A. *J. Phys. Org. Chem.* **2005**, *18*, 35–48.

(8) (a) Roux, M. V.; Dávalos, J. Z.; Jiménez, P.; Flores, H.; Saiz, J.-L.; Abboud, J.-L. M.; Juaristi, E. *J. Chem. Thermodyn.* **1999**, *31*, 635–646. (b) Dávalos, J. Z.; Flores, H.; Jiménez, P.; Notario, R.; Roux, M. V.; Juaristi, E.; Hosmane, R. S.; Liebman, J. F. *J. Org. Chem.* **1999**, *64*, 9328–9336. (c) Roux, M. V.; Jiménez, P.; Dávalos, J. Z.; Notario, R.; Juaristi, E. *J. Org. Chem.* **2001**, *66*, 5343–5351. (d) Roux, M. V.; Temprado, M.; Jiménez, P.; Dávalos, J. Z.; Notario, R.; Guzmán-Mejía, R.; Juaristi, E. *J. Org. Chem.* **2003**, *68*, 1762–1770. (e) Roux, M. V.; Temprado, M.; Jiménez, P.; Notario, R.; Guzmán-Mejía, R.; Juaristi, E. *J. Org. Chem.* **2004**, *69*, 1670–1675. (f) Roux, M. V.; Temprado, M.; Jiménez, P.; Dávalos, J. Z.; Notario, R.; Martín-Valcárcel, G.; Garrido, L.; Guzmán-Mejía, R.; Juaristi, E. *J. Org. Chem.* **2004**, *69*, 5454–5459.

(9) Spartan'04, v.1.0.1; Wave function Inc.: Irvine, CA 92612.

(10) Frisch, M. J.; Trucks, G. W.; Schlegel, H. B.; Scuseria, G. E.; Robb, M. A.; Cheeseman, J. R.; Montgomery, J. A., Jr.; Vreven, T.; Kudin, K. N.; Burant, J. C.; Millam, J. M.; Iyengar, S. S.; Tomasi, J.; Barone, V.; Mennucci, B.; Cossi, M.; Scalmani, G.; Rega, N.; Petersson, G. A.; Nakatsuji, H.; Hada, M.; Ehara, M.; Toyota, K.; Fukuda, R.; Hasegawa, J.; Ishida, M.; Nakajima, T.; Honda, Y.; Kitao, O.; Nakai, H.; Klene, M.; Li, X.; Knox, J. E.; Hratchian, H. P.; Cross, J. B.; Adamo, C.; Jaramillo, J.; Gomperts, R.; Stratmann, R. E.; Yazyev, O.; Austin, A. J.; Cammi, R.; Pomelli, C.; Ochterski, J. W.; Ayala, P. Y.; Morokuma, K.; Voth, G. A.; Salvador, P.; Dannenberg, J. J.; Zakrzewski, V. G.; Dapprich, S.; Daniels, A. D.; Strain, M. C.; Farkas, O.; Malick, D. K.; Rabuck, A. D.; Raghavachari, K.; Foresman, J. B.; Ortiz, J. V.; Cui, Q.; Baboul, A. G.; Clifford, S.; Cioslowski, J.; Stefanov, B. B.; Liu, G.; Liashenko, A.; Piskorz, P.; Komaromi, I.; Martin, R. L.; Fox, D. J.; Keith, T.; Al-Laham, M. A.; Peng, C. Y.; Nanayakkara, A.; Challacombe, M.; Gill, P. M. W.; Johnson, B.; Chen, W.; Wong, M. W.; Gonzalez, C.; Pople, J. A. *Gaussian 03*, revision B.05; Gaussian, Inc.: Pittsburgh, PA, 2003.

(11) Stephens, P. J.; Devlin, F. J.; Chabalowski, C. F.; Frisch, M. J. *J. Phys. Chem.* **1994**, *98*, 11623–11627.

(12) Becke, A. D. *J. Chem. Phys.* **1993**, *98*, 5648–5652.

(13) Lee, C.; Yang, W.; Parr, R. G. *Phys. Rev. B* **1988**, *37*, 785–789.

(14) Krishnan, R.; Binkley, J. S.; Seeger, R.; Pople, J. A. *J. Chem. Phys.* **1980**, *72*, 650–654.

(15) McLean, A. D.; Chandler, G. S. *J. Chem. Phys.* **1980**, *72*, 5639–5648.

(16) Clark, T.; Chandrasekhar, J.; Spitznagel, G. W.; Schleyer, P. v. R. *J. Comput. Chem.* **1983**, *4*, 294–301.

(17) Wiberg, K. B.; Castejon, H.; Bailey, W. F.; Ochterski, J. *J. Org. Chem.* **2000**, *65*, 1181–1187.

(18) Scott, A. P.; Radom, L. *J. Phys. Chem.* **1996**, *100*, 16502–16513.

(19) (a) Fukui, K. *Acc. Chem. Res.* **1981**, *14*, 363–368. (b) González, C.; Schlegel, H. B. *J. Phys. Chem.* **1990**, *94*, 5523–5527.

(20) Fernández-Alonso, M. C.; Cañada, J.; Jiménez-Barbero, J.; Cuevas, G. *ChemPhysChem* **2005**, *6*, 671–681.

(21) Fernández-Alonso, M. C.; Asensio, J. L.; Cañada, J.; Jiménez-Barbero, J.; Cuevas, G. *ChemPhysChem* **2003**, *4*, 754–757.

(22) Lowry, T. H.; Richardson, K. S. *Mechanism and Theory in Organic Chemistry*, 2nd ed.; Harper and Row: New York, 1981.

(23) Lambert, J. B.; Mixan, C. E.; Johnson, D. H. *J. Am. Chem. Soc.* **1973**, *95*, 4634–4639.

(24) Friebolin, H.; Kabuss, S.; Maier, W.; Lüttringhaus, A. *Tetrahedron Lett.* **1962**, 683–690.

(25) Perlin, A. S.; Casu, B. *Tetrahedron Lett.* **1969**, *10*, 2921–2924.

(26) Wolfe, S.; Pinto, B. M.; Varma, V.; Leung, R. Y. N. *Can. J. Chem.* **1990**, *68*, 1051–1062.

(27) (a) David, S. In *Anomeric Effect: Origin and Consequences*; Szarek, W. A., Horton, D., Eds.; American Chemical Society Symposium Series: Washington, DC, 1979. (b) Fraser, R. R.; Bresse, M. *Can. J. Chem.* **1983**, *61*, 576–578. See also: (c) Juaristi, E.; Cuevas, G. *Tetrahedron* **1992**, *48*, 5019–5087. (d) Juaristi, E.; Cuevas, G. *The Anomeric Effect*; CRC Publishers: Boca Raton, FL, 1992. (e) Additional effects such as dipole-induced dipole interactions are likely to contribute to the observed Perlin effects. See: Cuevas, G.; Martínez-Mayorga, K.; Fernández-Alonso, M.; Jiménez-Barbero, J.; Perrin, C. L.; Juaristi, E.; López-Mora, N. *Angew. Chem., Int. Ed.* **2005**, *44*, 2360–2364.

(28) (a) Bailey, W. F.; Rivera, A. D.; Rossi, K. *Tetrahedron Lett.* **1988**, *29*, 5621–5624. See also: (b) Juaristi, E.; Cuevas, G. *Tetrahedron Lett.* **1992**, *33*, 1847–1850. (c) Juaristi, E.; Cuevas, G.; Vela, A. *J. Am. Chem. Soc.* **1994**, *116*, 5796–5804.

(29) Wolfe, S.; Kim, C.-K. *Can. J. Chem.* **1991**, *69*, 1408–1412.

(30) (a) Malkin, V. G.; Malkina, O. L.; Casida, M. E.; Salahub, D. R. *J. Am. Chem. Soc.* **1994**, *116*, 5898–5908. (b) Malkina, O. L.; Salahub, D. R.; Malkin, V. G. *J. Chem. Phys.* **1996**, *105*, 8793–8800.

- (31) Cuevas, G.; Juaristi, E. *J. Am. Chem. Soc.* **2002**, *124*, 13088–13096.
- (32) (a) Wolfe, S.; Bernardi, F.; Csizmadia, I. G.; Mangini, A. In *Organic Sulfur Chemistry*; Elsevier: Amsterdam, 1985; pp 133–190. (b) Juaristi, E.; Ordóñez, M. In *Organosulfur Chemistry. Synthetic and Stereochemical Aspects*; Academic Press: London, 1998; pp 63–95.
- (33) (a) Alabugin, I. V. *J. Org. Chem.* **2000**, *65*, 3910–3919. (b) Alabugin, I. V.; Manoharan, M.; Zeidan, T. A. *J. Am. Chem. Soc.* **2003**, *125*, 14014–14031.

- (34) (a) Alabugin, I. V.; Manoharan, M.; Peabody, S.; Weinhold, F. *J. Am. Chem. Soc.* **2003**, *125*, 5973–5987. (b) Weinhold, F. Natural Bond Orbital Methods. In *Encyclopedia of Computational Chemistry*; Schleyer, P. v. R., Allinger, N. L., Clark, T., Gasteiger, J., Kollman, P. A., Schaefer, H. F., III, Schreiner, P. R., Eds.; Wiley: Chichester, UK, 1998; Vol. III, pp 1792–1811.
- (35) Juaristi, E.; Notario, R.; Roux, M. V. *Chem. Soc. Rev.* **2005**, *34*, 347–354.